

# Dipolar dephasing of Rydberg $D$ -state polaritons

C. Tresp,<sup>1,\*</sup> P. Bienias,<sup>2</sup> S. Weber,<sup>2</sup> H. Gorniaczyk,<sup>1</sup> I. Mirgorodskiy,<sup>1</sup> H. P. Büchler,<sup>2</sup> and S. Hofferberth<sup>1,†</sup>

<sup>1</sup>*Phys. Institut and Center for Integrated Quantum Science and Technology*

<sup>2</sup>*Institute for Theoretical Physics III and Center for Integrated Quantum Science and Technology, Universität Stuttgart, Pfaffenwaldring 57, 70569 Stuttgart, Germany*

We experimentally study the effects of the anisotropic Rydberg-interaction on  $D$ -state Rydberg polaritons slowly propagating through a cold atomic sample. In addition to the few-photon nonlinearity known from similar experiments with Rydberg  $S$ -states, we observe the interaction-induced dephasing of Rydberg polaritons at very low photon input rates into the medium. We develop a model combining the propagation of the two-photon wavefunction through our system with nonperturbative calculations of the anisotropic Rydberg-interaction to show that the observed effect can be attributed to pairwise interaction of individual Rydberg polaritons.

Long-range and spatially anisotropic dipole-dipole (DD) interactions enable new approaches for preparing and exploring strongly correlated quantum systems [1]. Magnetic DD interaction couples individual nuclear spins to nitrogen-vacancy centers in diamond [2, 3] and is observed in dipolar gases of ultracold atoms [4, 5]. Electric DD interaction determines the long-range interaction between polar molecules [6] or Rydberg atoms [7, 8] and may allow to investigate phenomena such as quantum magnetism [9–11] and topological phases [12] in these systems. Recently the angular dependence of the DD interaction between single Rydberg atoms has been fully mapped [13]. Here we study, for the first time, the anisotropic DD interaction between slowly travelling polaritons coupled to a Rydberg  $D$ -state via electromagnetically-induced transparency (EIT) [14].

Rydberg-EIT has emerged as a powerful approach to realizing few-photon optical nonlinearities [15–18]. This novel technique enables a variety of optical quantum information applications such as highly efficient single-photon generation [19], entanglement generation between light and atomic excitations [20], single-photon all-optical switches [21] and transistors [22, 23], and interaction-induced photon phase shifts [24]. Additionally, it allows us to probe novel phenomena such as attractive interaction between single photons [25], crystallization of photons [26], or photonic scattering resonances [27]. The electric DD interaction between pairs of Rydberg atoms has been studied extensively in the perturbative van-der-Waals regime [28–30]. Rydberg-EIT experiments have so far mostly employed Rydberg  $S$ -states, where the interaction has only very weak angular dependence. Recent experiments have employed additional microwave or light fields to simultaneously prepare Rydberg atoms in  $S$ - and  $P$ -states [31] or two different  $S$ -states [22, 23, 32]. The interaction between these energetically well-separated states enables novel entanglement schemes for atomic systems [33] and increased flexibility in the manipulation of weak light fields [34, 35]. For Rydberg states with non-zero orbital angular momentum coupling terms between the degenerate Zeeman sublevels become relevant [29, 30].

In this work, we study the decoupling of Rydberg polaritons from the EIT control field due to anisotropic interaction as an effect beyond the blockade-mediated few-photon nonlinearity [18]. We show that this dephasing is significant for incident probe photon rates corresponding to a mean number of less than two polaritons inside the medium and extract the scaling of the dephasing rate with EIT control Rabi frequency and principal quantum number of the Rydberg  $D$ -state. Finally, we present a model which combines dephasing rates extracted from nonperturbatively calculated pair potentials with numerical propagation of the two-polariton wavefunction to describe our experimental observations.

Our EIT scheme consists of a few photon probe field  $\mathcal{E}_p$  and a strong coupling field  $\Omega$  resonantly coupling the levels illustrated in Fig. 1(a). Resulting transmission spectra of  $\mathcal{E}_p$  for a frequency scan of the probe laser over EIT resonance employing the  $|80D_{5/2}\rangle$  Rydberg state for two different photon rates  $R_{in}$  are shown in Fig. 1(b). For  $R_{in} = 0.15$  photons/ $\mu$ s we reach high transmission and a narrow linewidth, from which we extract a decoherence rate  $\gamma_{gr} = 2\pi \cdot 200$  kHz, originating from the movement of the atoms due to the finite temperature and stray electric and magnetic fields over the cloud. For higher probe input rates the EIT transmission decreases, due to the self-blockade of propagating polaritons as observed in experiments using Rydberg  $S$ -states [16, 18, 19]. We observe a qualitative difference to these experiments when we measure the time dependence of the transmission on EIT resonance (Fig. 1(d)). For very low photon rates on the order of  $R_{in} = 0.15$  photons/ $\mu$ s where we rarely have two photons inside the medium, we measure a constant transmission, which is determined by  $\Omega$  and the decoherence rate  $\gamma_{gr}$ . If we increase  $R_{in}$ , we find a non-linear decrease of initial transmission, which is caused by the blockade-induced nonlinearity. On top of this, we observe a decay of transmission over time which gets faster with increasing rate  $R_{in}$ . Latest we solely observe when using Rydberg  $D$ -states in our EIT scheme. We attribute this effect to interaction-induced coupling to degenerate Zeeman sublevels which leads to polaritons being converted to stationary Rydberg excitations inside

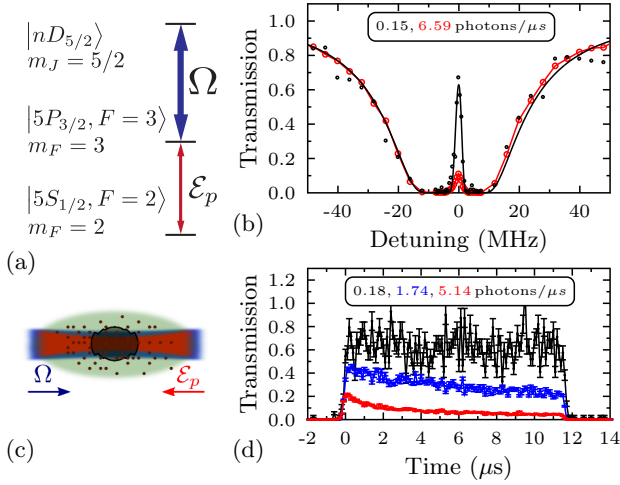


FIG. 1. (a) EIT level scheme with weak probe field  $\mathcal{E}_p$  and strong control field  $\Omega$ . (b) Frequency scan of the weak probe field  $\mathcal{E}_p$  showing the EIT transmission window averaged over the full pulse time. The transmission shows a strong nonlinearity with incident photon rate. (c) Geometric scheme of our setup consisting of EIT lasers at 780 nm ( $w_0 \approx 6 \mu\text{m}$ ) and 480 nm ( $w_0 \approx 12 \mu\text{m}$ ) focused onto a thermal cloud (30  $\mu\text{K}$ ) of  $^{87}\text{Rb}$  atoms with extensions of  $\sigma_z = 80 \mu\text{m}$  and  $\sigma_r = 25 \mu\text{m}$ . The grey shadow shows the anisotropic blockade region caused by a  $|100D_{5/2}\rangle$  Rydberg excitation. (d) Time dependent transmission on two-photon resonance for different probe photon input.

the cloud. These impurities shift the Rydberg levels of the surrounding atoms, preventing other polaritons from propagating through the cloud [21–23].

To investigate the dependence of the decay of transmission on the photon rate  $R_{in}$ , we calculate an effective optical depth ( $OD_{eff}$ ) of our medium on EIT resonance ( $\Delta = 0$ ) by taking the logarithm of the transmission (Fig. 2(a)). To account for the three effects described above, we write  $OD_{eff}$  as

$$OD_{eff} = OD_{dec} + OD_{sat}(R_{in}) + OD_{dph}(R_{in}, t), \quad (1)$$

where the terms  $OD_{dec}$ ,  $OD_{sat}$  and  $OD_{dph}$  represent the contributions of decoherence, saturation, and dephasing.

Neglecting saturation effects for the highest values of  $R_{in}$ , we approximate the increase in  $OD$  due to dephasing to be linear in time and write  $OD_{dph} = R_{OD} \cdot t$ , with  $R_{OD}$  as creation rate of optical density due to dephasing.

In Fig. 2(b) the extracted rates  $R_{OD}$  are plotted versus  $R_{in}$  for measurements with different control field Rabi frequencies  $\Omega$  coupling to the  $|88D_{5/2}, m_J = 5/2\rangle$  state. For measurements with  $\Omega = 2\pi \cdot 16.6 \text{ MHz}$  and  $\Omega = 2\pi \cdot 26.3 \text{ MHz}$ , respectively,  $R_{OD}$  scales quadratically with  $R_{in}$ . For  $\Omega = 2\pi \cdot 6.1 \text{ MHz}$  and  $\Omega = 2\pi \cdot 10.8 \text{ MHz}$  we see deviations from the quadratic dependence for  $R_{in}$  exceeding 1.5 and 2.3, respectively. Comparing these

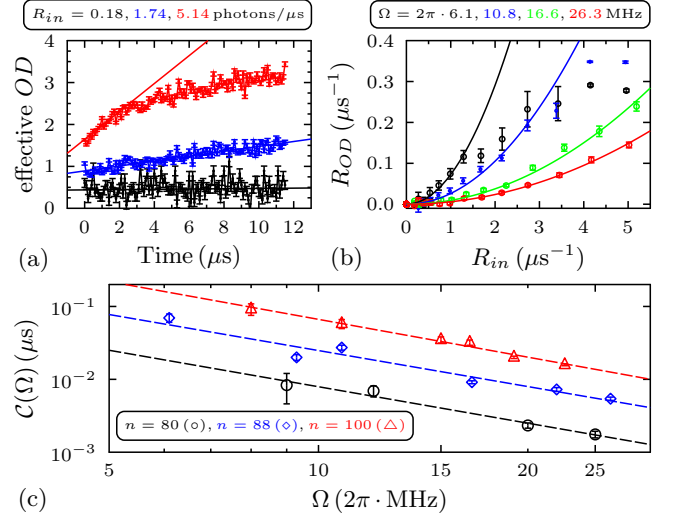


FIG. 2. (a) Effective optical density of the  $|88D_{5/2}\rangle$  EIT feature for different photon rates at fixed  $\Omega = 2\pi \cdot 8.3 \text{ MHz}$ . The solid lines are linear fits to the data to extract the rates  $R_{OD}$  of additional  $OD_{eff}$  due to the creation of impurities. (b) Dependence of  $R_{OD}$  on  $R_{in}$  for different Rabi frequencies  $\Omega$ . Parabolic fits (solid lines) determine the rate constant  $\mathcal{C}(\Omega)$  for each dataset. (c) Rate constants  $\mathcal{C}$  for different  $\Omega$ . For the different principal quantum numbers  $n$  we observe the same scaling according to Eq. (3) with  $k = 1.67(4)$ . Dashed lines are fits to the data.

rates to the delay time in the medium given by  $\tau_{delay} = \frac{OD \cdot \gamma_e}{2\Omega^2}$  (where  $\gamma_e = 2\pi \cdot 6.1 \text{ MHz}$  is the decay rate of intermediate state  $|5P_{3/2}\rangle$ ), we start to see deviations from the quadratic dependence when the mean number of photons in the medium exceeds 2. This quadratic dependence of  $R_{OD}$  on  $R_{in}$  suggests that the observed dephasing is a two-body effect. In particular, we will later relate the dephasing to the probability  $|\psi_{dd}|^2$  of finding two polaritons in the Rydberg state at the same time for distances larger than the blockade radius  $r_b$ , given by

$$|\psi_{dd}|^2 = \frac{R_{in}^2}{v_g^2}. \quad (2)$$

Because of this dependence, we introduce a rate constant  $\mathcal{C}(\Omega)$ , relating  $R_{OD}$  and  $R_{in}$  in the quadratic regime via  $R_{OD} = \mathcal{C}(\Omega) \cdot R_{in}^2$ , which we obtain from fits to our data (Fig. 2(b)).

The  $\Omega$  dependence of the extracted rate constants is shown in Fig. 2(c) for measurements with principal quantum numbers  $n = 80$ ,  $n = 88$  and  $n = 100$ . To compare the results for different principal quantum numbers, we extract the dependence on  $\Omega$  by a fit of the form

$$\mathcal{C}(\Omega) = a \cdot \Omega^{-k}, \quad (3)$$

which yields  $k = 1.67(4)$  for all the different  $n$ . However, for the prefactor  $a$  we observe a strong scaling with  $n$ , indicating significantly larger dephasing for larger  $n$ .

In order to connect our observations to the anisotropy of the Rydberg interaction we calculate Rydberg pair potentials through diagonalization of the electrostatic DD interaction Hamiltonian [36]. To reduce computation time we diagonalize the Hamiltonian in the coordinate system aligned with the atomic separation, where the total magnetic moment  $M = m_{J1} + m_{J2}$  is conserved. The angular dependence of the interaction is accounted for by rotating the pair states from the fixed coordinate system defined by the direction of light propagation into the interatomic coordinate system by means of Wigner d-matrices [29]. Calculated pair potentials for  $|80D_{5/2}; 80D_{5/2}\rangle$  and  $|100D_{5/2}; 100D_{5/2}\rangle$  are shown in Fig. 3(a) and (b). The colored shadow of the potentials presents the projection of the  $|nD_{5/2}, m_J = 5/2; nD_{5/2}, m_J = 5/2\rangle$  pair state in the fixed coordinate system on the new eigenstates for an angle  $\theta = 60^\circ$  between the interatomic axis and the light propagation direction. It can be seen that this originally unperturbed state is projected onto multiple new eigenstates. Unlike for isotropic  $S$ -states this projection depends strongly on the angle  $\theta$  [29]. In other words, the magnetic quantum number  $m_{J1}$  and  $m_{J2}$  of individual Rydberg polaritons are no longer good quantum numbers when interaction is taken into account [28]. One consequence of the anisotropic interaction is that the blockade volume for  $D$ -states is not spherical as the interaction potential can no longer be described by a single  $C_6$  coefficient. Secondly, the splitting of the single pair state into several lines induces a time evolution of the polariton pair out of the initial state, resulting in the observed decoupling of Rydberg polaritons.

For a more quantitative analysis of this effect, we combine the full potential calculation with photon propagation under EIT. In the weak-probe limit, it is sufficient to consider only two photons simultaneously inside the medium [18, 27]. Then, the interaction between the Rydberg states is responsible for two phenomena: first, it leads to an effective interaction potential between the slow light polaritons  $V(z, r_\perp)$ , and second, it couples degenerate Zeeman-states in the  $D_{5/2}$ -manifold (Fig. 4(a)). The latter leads to an effective decay of the Rydberg polaritons into localized Rydberg excitations, which we account for by an effective decay rate  $\Gamma(z, r_\perp)$ . Here,  $z = z_1 - z_2$  and  $r_\perp = r_{\perp,1} - r_{\perp,2}$  are the relative coordinate along and perpendicular to the propagation direction. In order to incorporate both phenomena into our analysis, we calculate the time evolution of a stationary Rydberg pair initially in the Zeeman pair state  $|m_{J1,2} = 5/2, 5/2\rangle$  at given distance and angle between light propagation direction and interatomic axis from the full interaction potential. Although this dynamics is fully coherent, the revival of the initial population appears only on time scales long compared to the polariton propagation time due to the large number of states in the  $D$ -state manifold. Hence, the initial time evolution on

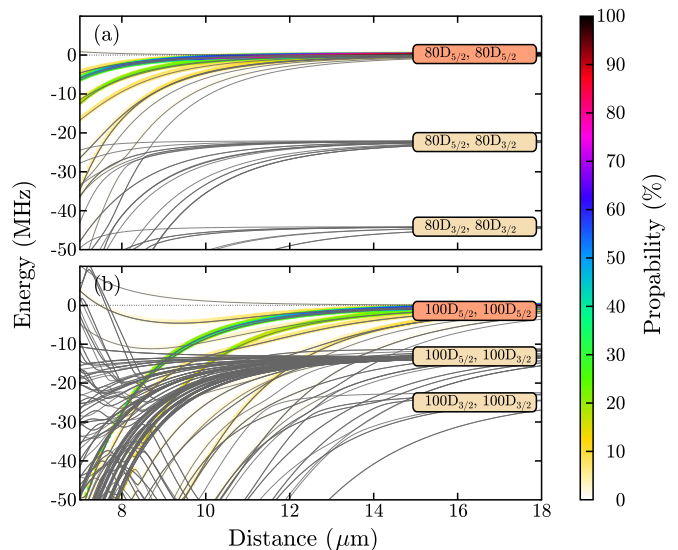


FIG. 3. Calculated pair state potentials of (a)  $|80D_{5/2}; 80D_{5/2}\rangle$  and (b)  $|100D_{5/2}; 100D_{5/2}\rangle$  pair states. The color code represents the projection of the initial  $|m_{J1,2} = 5/2, 5/2\rangle$  state for an angle of  $\theta = 60^\circ$  (between the interatomic axis and the light propagation direction) on the new eigenstates.

experimentally relevant time scales is well described by a spatially varying dephasing rate  $\Gamma(z, r_\perp)$  (Fig. 4(b)). The important fact here is that for  $D$ -states  $\Gamma(z, r_\perp)$  is large at distances beyond the blockade volume. In contrast, the same approach results in vanishingly small dephasing rates for  $S$ -states.

For the propagation dynamics we solve numerically the full set of propagation equations for the two-body wave function [18, 25]. Comparing with  $S$ -state calculations we now include the dephasing rate  $\Gamma(z, r_\perp)$  as a decay of the amplitude  $\psi_{dd}(\mathbf{r}_1, \mathbf{r}_2)$  of two Rydberg excitations. We assume a homogeneous distribution of atoms inside the finite-size medium of length  $L = 4\sigma_z$  and include imperfect single-photon transmission due to the decoherence  $\gamma_{gr}$  of the 2-photon transition. Neglecting probe-beam diffraction due to the interaction, we solve polariton dynamics (Fig. 4(c)) for different  $r_\perp$  with  $V_{1D}(z) = V(z, r_\perp)$  followed by averaging over the  $r_\perp$  distribution determined by the Gaussian transverse profile with waist  $w_{eff} = 7\mu m$  (corresponding to the waist averaged over length  $L$ ) of the probe beam.

Then, the rate of events  $\mathcal{N}$  that at least one photon is converted into stationary Rydberg excitation is proportional to the amplitude of the two-polariton wavefunction  $\psi_{dd}$ :

$$\mathcal{N} = \int_V d\mathbf{r}_1 d\mathbf{r}_2 \Gamma(\mathbf{r}_1 - \mathbf{r}_2) |\psi_{dd}(\mathbf{r}_1, \mathbf{r}_2)|^2. \quad (4)$$

Note, that we normalize the Rydberg wave function  $\psi_{dd}$  with the incoming photon flux as in Eq. (2).

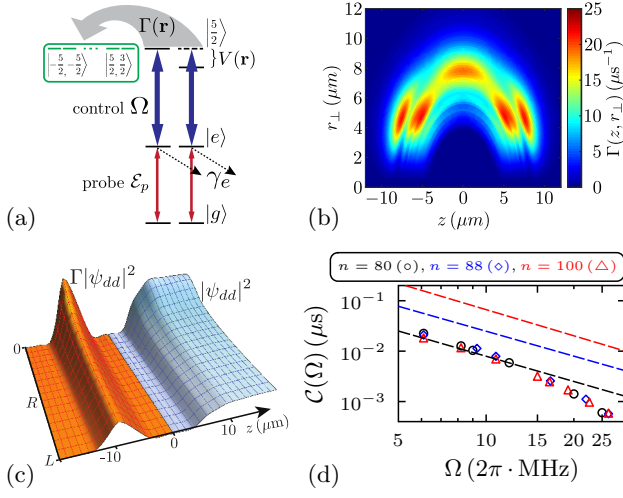


FIG. 4. (a) Dipolar interaction leads to the energy shift  $V(\mathbf{r})$  of  $|5/2, 5/2\rangle$  state, with  $\mathbf{r} = (z, r_\perp)$ , and also to evolution from initial  $|5/2\rangle$  into  $m_J \neq 5/2$  states described by the position dependent decay rate  $\Gamma(\mathbf{r})$ . We neglect control field coupling of  $m_J \neq 5/2$  to corresponding  $5P_{3/2}$ -levels. (b) Dephasing rate out of  $|5/2, 5/2\rangle$  state for  $n = 80$ . (c) Numerical simulations showing: For  $z > 0$  probability distribution associated with two Rydberg excitations  $|\psi_{dd}(z, R)|^2$ . For  $z < 0$  the product  $\Gamma(z)|\psi_{dd}(z, R)|^2$ , where  $R = (z_1 + z_2)/2$  is the center of mass coordinate. Both quantities are presented in arbitrary units for  $r_\perp = 4.2\mu\text{m}$ ,  $\Omega = 2\pi \cdot 12\text{ MHz}$ ,  $n = 80$  and probe-beam waist  $w_{\text{eff}} = 7\mu\text{m}$ . (d) Comparison of  $\mathcal{C}(\Omega)$  from numerical simulations (circles) with fits to experimental data from Fig. 2(c) (dashed lines).

A single dephasing event increases on average the optical depth within the medium by  $OD_{im}$  for the incoming photons. Therefore, the change in transmission by a single dephasing event is  $\exp(-OD_{dec} - OD_{sat}(R_{in}))(1 - e^{-OD_{im}})$ . This reduction appears with the rate  $\mathcal{N}$ , and therefore the initial time evolution for the averaged transmission behaves as

$$T(t) = e^{-OD_{dec} - OD_{sat}(R_{in})} \exp[-\mathcal{N}t(1 - e^{-OD_{im}})] \quad (5)$$

and leads to a rate constant  $\mathcal{C}(\Omega) = \mathcal{N}(1 - e^{-OD_{im}})/R_{in}^2$ . Furthermore, we observe, that a finite life time of the Rydberg impurity results in an effective saturation of the transmission. However, the full time evolution for the transmission including higher number of excited Rydberg impurities is extremely challenging and beyond the scope of the present manuscript.

These calculations provide important insights into the behavior of the dephasing. First, the averaged optical thickness  $OD_{im} > 1$  of a dephasing event is sufficient to strongly block the medium. Therefore, the decay mainly follows the probability to absorb at least one impurity. Second, there appears a characteristic distance with the highest probability for the excitation of an impurity Rydberg state given by the competition between

the higher dephasing rates at shorter distances and the suppression to find two Rydberg excitations due to the blockade effect, Fig. 4(b-c). The latter is strongly affected by the polariton dynamics inside the medium, as has been previously discussed in terms of a diffusive behavior [18]: at the entrance of the two photons into the medium, the probability to find two Rydberg excitations is purely determined by the blockade due to interactions  $\psi_{dd}(z) \sim 1/(1 - \bar{\chi}V_{1D}(z))$  where  $\hbar\bar{\chi} = -i(\gamma_e/\Omega^2 + 1/\gamma_e)$  [27]. This dip in probability broadens during propagation due to correction to the linear behavior of the polariton dispersion, while the single polariton losses provide an overall reduction of the amplitude (see Fig. 4(c)). Those effects strongly depend on  $\Omega$ . In addition, photons inside the medium are compressed due to the slow light velocity, which contributes an additional factor  $\Omega^{-4}$  (Eq. (2)) to the scaling of  $\mathcal{C}(\Omega)$  with  $\Omega$ . Both described effects combined explain the numerical results presented in Fig. 4(d). We find qualitative agreement between theory and experiment without any fitting parameters. While for low  $n$  and small values of  $\Omega$  the agreement is excellent, for larger  $\Omega$  we observe a discrepancy, and moreover, the theory does not reproduce the strong scaling with main principal quantum number  $n$  measured in the experiment. We expect the following phenomena to be the reason for this discrepancy. First, the theoretical analysis does not include the control field coupling of  $m_J \neq 5/2$  states to  $5P_{3/2}$  manifold, which provides AC-stark shift and broadening of the Rydberg lines. Furthermore, the splitting between the  $nD_{5/2}$  and  $nD_{3/2}$  manifold, which scales with  $n^{-3}$  is reduced and eventually becomes comparable to  $\Omega$  and  $\gamma_e$ . Thus, the  $nD_{3/2}$  manifold will impact evolution of the system and this effect will be stronger for higher  $n$  and  $\Omega$ .

In summary, we have investigated the effect of anisotropic DD interaction between Rydberg  $D$ -state polaritons. Interaction-induced decoupling into stationary Rydberg excitations results in a decrease of transmission on EIT resonance over time. This effect is relevant to all Rydberg-EIT experiments employing non- $S$ -states [31] or Förster resonances [23, 32], where the anisotropy of the Rydberg interaction will always result in coupling to additional levels. Our theoretical approach to include full Rydberg pair state potentials in numerical two-photon propagation in the form of an effective potential and anisotropic decay rate yields qualitative agreement with our measurements and thus is a useful tool for treating complex Rydberg polariton interaction in general. The fact that we observe the interaction-induced state-mixing on the few-photon level is a promising result for experiments on Rydberg-dressing [10, 11] and engineered polariton-interaction [37] using Rydberg states with orbital angular momentum. More detailed study of the anisotropic coupling will be possible in storage and retrieval experiments [21, 38], enabling control over number and position of stored excitations. In this scenario, it be-



comes particularly interesting to employ echo techniques [39] to probe the coherent spin evolution of interacting Rydberg-polaritons.

We thank Rick van Bijnen for important input in developing the core idea of this work and Thomas Pohl for helpful discussions. This work is funded by the German Research Foundation (DFG) through Emmy-Noether-grant HO 4787/1-1 and within SFB/TRR21. HG acknowledges support from the Carl-Zeiss Foundation, PB from EU Marie Curie ITN COHERENCE.

---

\* [c.tresp@physik.uni-stuttgart.de](mailto:c.tresp@physik.uni-stuttgart.de)

† [s.hofferberth@physik.uni-stuttgart.de](mailto:s.hofferberth@physik.uni-stuttgart.de)

- [1] T. Lahaye, C. Menotti, L. Santos, M. Lewenstein, and T. Pfau, *Reports on Progress in Physics* **72**, 126401 (2009).
- [2] M. V. G. Dutt, L. Childress, L. Jiang, E. Togan, J. Maze, F. Jelezko, A. S. Zibrov, P. R. Hemmer, and M. D. Lukin, *Science* **316**, 1312 (2007).
- [3] P. Neumann, N. Mizuochi, F. Rempp, P. Hemmer, H. Watanabe, S. Yamasaki, V. Jacques, T. Gaebel, F. Jelezko, and J. Wrachtrup, *Science* **320**, 1326 (2008).
- [4] T. Lahaye, T. Koch, B. Froehlich, M. Fattori, J. Metz, A. Griesmaier, S. Giovanazzi, and T. Pfau, *Nature* **448**, 672 (2007).
- [5] K. Aikawa, S. Baier, A. Frisch, M. Mark, C. Ravensbergen, and F. Ferlaino, *Science* **345**, 1484 (2014).
- [6] B. Yan, S. A. Moses, B. Gadway, J. P. Covey, K. R. A. Hazzard, A. M. Rey, D. S. Jin, and J. Ye, *Nature* **501**, 521 (2013).
- [7] D. Comparat and P. Pillet, *J. Opt. Soc. Am. B* **27**, A208 (2010).
- [8] M. Saffman, T. G. Walker, and K. Mølmer, *Rev. Mod. Phys.* **82**, 2313 (2010).
- [9] A. V. Gorshkov, S. R. Manmana, G. Chen, J. Ye, E. Demler, M. D. Lukin, and A. M. Rey, *Phys. Rev. Lett.* **107**, 115301 (2011).
- [10] A. W. Glaetzle, M. Dalmonte, R. Nath, C. Gross, I. Bloch, and P. Zoller, *Phys. Rev. Lett.* **114**, 173002 (2015).
- [11] R. M. W. van Bijnen and T. Pohl, (2014), [arXiv:1411.3118v1](https://arxiv.org/abs/1411.3118v1) [cond-mat.quant-gas].
- [12] N. Y. Yao, C. R. Laumann, A. V. Gorshkov, S. D. Bennett, E. Demler, P. Zoller, and M. D. Lukin, *Phys. Rev. Lett.* **109**, 266804 (2012).
- [13] S. Ravets, H. Labuhn, D. Barredo, T. Lahaye, and A. Browaeys, (2015), [arXiv:1504.00301](https://arxiv.org/abs/1504.00301) [physics.atom-ph].
- [14] M. Fleischhauer and M. D. Lukin, *Phys. Rev. Lett.* **84**, 5094 (2000).
- [15] I. Friedler, D. Petrosyan, M. Fleischhauer, and G. Kurizki, *Phys. Rev. A* **72**, 043803 (2005).
- [16] J. D. Pritchard, D. Maxwell, A. Gauguier, K. J. Weatherill, M. P. A. Jones, and C. S. Adams, *Phys. Rev. Lett.* **105**, 193603 (2010).
- [17] A. V. Gorshkov, J. Otterbach, M. Fleischhauer, T. Pohl, and M. D. Lukin, *Phys. Rev. Lett.* **107**, 133602 (2011).
- [18] T. Peyronel, O. Firstenberg, Q. Liang, S. Hofferberth, A. Gorshkov, T. Pohl, M. Lukin, and V. Vuletic, *Nature* **488**, 57 (2012).
- [19] Y. O. Dudin and A. Kuzmich, *Science* **336**, 887 (2012).
- [20] L. Li, Y. O. Dudin, and A. Kuzmich, *Nature* **498**, 466 (2013).
- [21] S. Baur, D. Tiarks, G. Rempe, and S. Dürr, *Phys. Rev. Lett.* **112**, 073901 (2014).
- [22] H. Gorniaczyk, C. Tresp, J. Schmidt, H. Fedder, and S. Hofferberth, *Phys. Rev. Lett.* **113**, 053601 (2014).
- [23] D. Tiarks, S. Baur, K. Schneider, S. Dürr, and G. Rempe, *Phys. Rev. Lett.* **113**, 053602 (2014).
- [24] V. Parigi, E. Bimbard, J. Stanojevic, A. J. Hilliard, F. Nogrette, R. Tualle-Brouiri, A. Ourjoumtsev, and P. Grangier, *Phys. Rev. Lett.* **109**, 233602 (2012).
- [25] O. Firstenberg, T. Peyronel, Q. Liang, A. V. Gorshkov, M. D. Lukin, and V. Vuletic, *Nature* **502**, 71 (2013).
- [26] J. Otterbach, M. Moos, D. Muth, and M. Fleischhauer, *Phys. Rev. Lett.* **111**, 113001 (2013).
- [27] P. Bienias, S. Choi, O. Firstenberg, M. F. Maghrebi, M. Gullans, M. D. Lukin, A. V. Gorshkov, and H. P. Büchler, *Phys. Rev. A* **90**, 053804 (2014).
- [28] K. Singer, J. Stanojevic, M. Weidemüller, and R. Cote, *J. Phys. B: At. Mol. Opt. Phys.* **38**, S295 (2005).
- [29] T. G. Walker and M. Saffman, *Phys. Rev. A* **77**, 032723 (2008).
- [30] B. Vermersch, A. W. Glaetzle, and P. Zoller, *Phys. Rev. A* **91**, 023411 (2015).
- [31] D. Maxwell, D. J. Szwer, D. Paredes-Barato, H. Busche, J. D. Pritchard, A. Gauguier, K. J. Weatherill, M. P. A. Jones, and C. S. Adams, *Phys. Rev. Lett.* **110**, 103001 (2013).
- [32] G. Guenter, H. Schempp, M. R. de Saint-Vincent, V. Gavryusev, S. Helmrich, C. S. Hofmann, S. Whitlock, and M. Weidemüller, *Science* **342**, 954 (2013).
- [33] D. Cano and J. Fortágh, *Phys. Rev. A* **89**, 043413 (2014).
- [34] W. Li, D. Viscor, S. Hofferberth, and I. Lesanovsky, *Phys. Rev. Lett.* **112**, 243601 (2014).
- [35] Y.-M. Liu, X.-D. Tian, D. Yan, Y. Zhang, C.-L. Cui, and J.-H. Wu, *Phys. Rev. A* **91**, 043802 (2015).
- [36] A. Schwettmann, J. Crawford, K. R. Overstreet, and J. P. Shaffer, *Phys. Rev. A* **74**, 020701 (2006).
- [37] M. F. Maghrebi, N. Y. Yao, M. Hafezi, T. Pohl, O. Firstenberg, and A. V. Gorshkov, *Phys. Rev. A* **91**, 033838 (2015).
- [38] Y. O. Dudin, L. Li, F. Bariani, and A. Kuzmich, *Nature Phys.* **8**, 790 (2012).
- [39] R. Kimmich, *NMR Tomography, Diffusometry, Relaxometry* (Springer, 2001).